Decadal variations in the Subtropical Cells and equatorial Pacific SST

Masami Nonaka[1], Shang-Ping Xie, and Julian P. McCreary

International Pacific Research Center/SOEST, University of Hawaii, Honolulu, Hawaii

Abstract. A mechanism for generating decadal sea surface temperature (SST) variability in the equatorial Pacific is investigated using an ocean general circulation model forced by observed wind stress. Equatorial SST variability is governed by different ocean dynamics on interannual and decadal time scales. At interannual time scales, equatorial SST anomalies are mainly driven by equatorial winds. At decadal time scales, on the other hand, they are forced both by equatorial winds and by off-equatorial winds in the tropics, while the contribution from midlatitude winds poleward of 25° is negligible. Trade-wind variations in the off-equatorial tropics force equatorial SST variability by spinning up and down the subtropical cells that transport cold water into the equatorial upwelling zone. Equatorial SST anomalies induced by this mechanism lag behind the response to local equatorial winds by about two years.

1. Introduction

Equatorial Pacific sea surface temperature (SST) is of central importance to global climate, for example, as in the interannually varying El Niño and the Southern Oscillation (ENSO) phenomenon. In addition to ENSO, eastern equatorial Pacific SST anomalies (SSTAs) also display significant decadal/interdecadal variations that modulate the amplitude and frequency of ENSO [*An and Wang*, 2000; *Fedorov and Philander*, 2000]. The leading empirical orthogonal function of Pacific SST variability on decadal time scales resembles that of interannual ENSO, but the equatorial center of action is weaker and has a much broader meridional scale [*Zhang et al.*, 1997].

The cause of decadal SSTAs in the equatorial Pacific is not yet clear. Some argue that the nonlinearity of the tropical ocean-atmosphere can, by itself, give rise to chaotic modulation of ENSO on decadal and longer time scales without involving the extratropics [*Timmermann and Jin*, 2001]. Noting that the sharp equatorial thermocline is maintained by transport of cold water subducted in the subtropics (Fig. 1), others suggest that variability of the shallow meridional overturning circulations, the Subtropical Cells (STCs; *McCreary and Lu*, 1994; *Liu*, 1994), play a key role through either of the following mechanisms: *i)* advection to the equator of temperature anomalies formed by subtropical subduction [*Gu and Philander*, 1997; *Zhang et al.*, 1998]; or *ii)* changes in STC strength, which cause equatorial SSTAs by varying the amount of the cold water that is transported into the tropics [*Kleeman et al.*, 1999]. Hereafter, we refer to the two STC processes as the $\overline{V}T'$ and the $V'\overline{T}$ mechanisms, respectively. These mechanisms may also work in the Atlantic, which also has STCs [*e.g.*, *Inui et al.*, 2001].

Recent studies suggest that the $V'\overline{T}$ mechanism is more viable than $\overline{V}T'$. For example, although the $\overline{V}T'$ mechanism is important for generating subsurface variability in the subtropical gyre [*Deser et al.*, 1996], modeling results suggest that it does not significantly affect equatorial temperature [*Schneider et al.*, 1999], as observed subtropical SSTAs are severely weakened by mixing before they reach the equator [*Nonaka and Xie*, 2000]. Conversely, in their analysis of historical hydrographic data, *McPhaden and Zhang* [2001] report a gradual increase in equatorial SST in recent decades and a simultaneous decrease in the equatorward geostrophic transport across 9°S and 9°N, consistent with the $V'\overline{T}$ mechanism.

The preceding ideas are based on simple coupled ocean-atmosphere models, and they are currently poorly constrained by ocean observations because the available records are too short in time and too coarse in space. In this paper, we investigate them further using an ocean general circulation model (GCM) of the Pacific. Specifically, we ask: Are the same ocean dynamics responsible for SST variability on both interannual and decadal time scales? Can off-equatorial forcing significantly influence equatorial decadal variability, and if so by what mechanism? The answers to these questions constrain theoretical possibilities.

The GCM we use is Modular Ocean Model version 1.1. It is forced by observed wind stress for 1958–97 [*Kalnay et al.*, 1996], and the SST and sea-surface-salinity (SSS) fields are restored toward observed monthly climatologies with a time constant of $\gamma = 1/14$ days^{-1} for the top 10-m water column. See *Xie et al.*, [2000] for details of the model set up. The use of surface restoring boundary conditions eliminates anomalous atmospheric thermal forcing, so that ocean dynamics are responsible for all the model's temperature variability. As a result, the model's SST variability is greatly reduced in the central and eastern North Pacific, where the atmospheric thermal forcing (by wind-induced evaporation, for example) is important [*Alexander et al.*, 2001]. Thus, the $\overline{V}T'$ mechanism in the model is essentially eliminated.

2. Equatorial SSTAs

Fig. 2A shows annual-mean equatorial SSTAs averaged from 140°W–90°W and 1°S–1°N (T'_{eq}), a region chosen because of its large decadal SST variability, both for the solution forced by the full observed winds (the "control" run hereafter; red curves) and for observations (black). Observed SSTAs have a warming trend larger than that in the

[1]Also Frontier Research System for Global Change, Yokohama, Japan

Paper number 1999GL000000.
0094-8276/01/1999GL000000$05.00

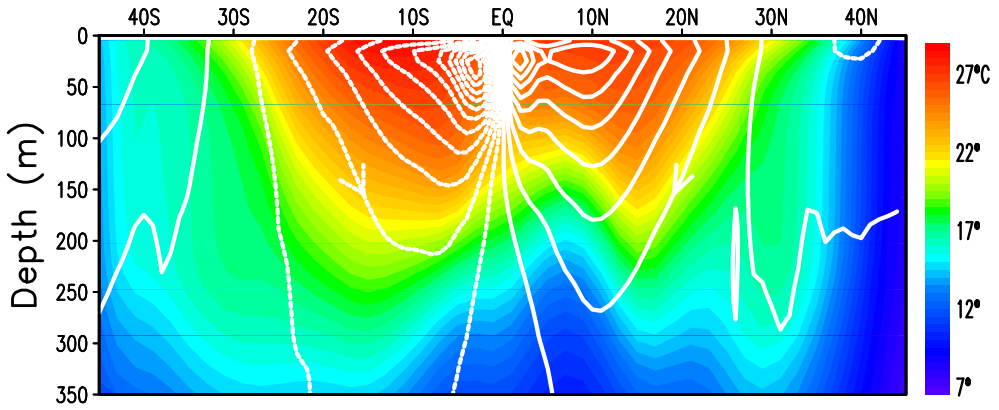

Figure 1. Latitude-depth section of mean ocean temperature $\overline{T}$ (color) at 170°W and meridional streamfunction $\overline{\psi}$ (contours) for the control run.

solution, and the trends are removed for easier comparison in all the following analyses. The time series successfully captures all the El Niño events (1965, 69, 72, 76, 83 and 92). This is not surprising because ENSO SSTAs are known to be caused by ocean dynamics, with atmospheric thermal forcing acting as a damping. While the decadal anomalies (thick curves) are not perfectly reproduced, the solution captures the rapid increase in equatorial SST in the mid-1970s and a cooling dip that bottomed in 1989. The relatively large discrepancy before 1980 between the two filtered curves may be due to errors in the forcing wind data.

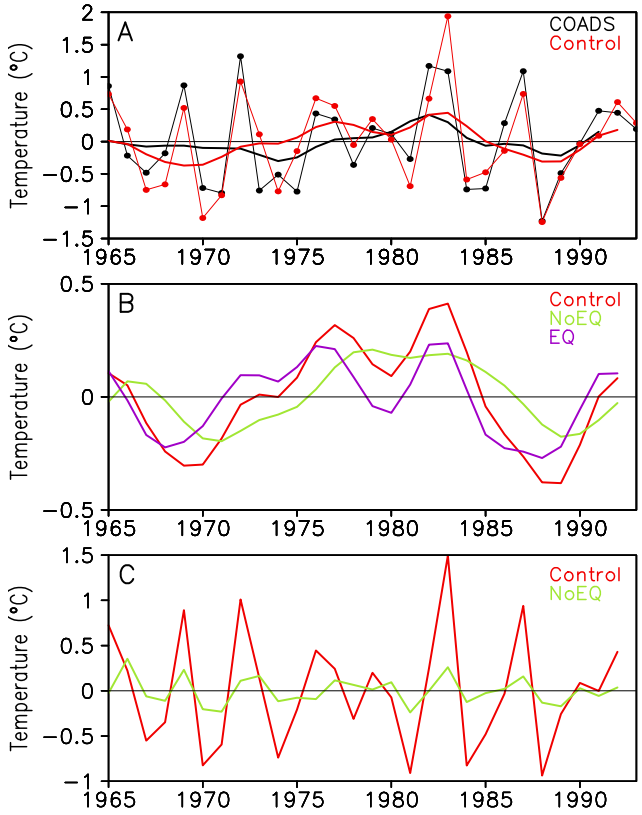

Figure 2. (A) Observed annual-mean (thin lines with dots) and decadal (thick lines) SST anomalies from the Comprehensive Ocean Atmosphere Data Set (black curves) and temperature anomalies from the control run at 15 m (red) in the eastern equatorial region (140–90°W, 1°S–1°N). The decadal curves are obtained by applying a 9-year, weighted, running-mean filter. (B) As in (A), except showing decadal anomalies for the control run (red) and the NoEQ (green) and EQ (purple) solutions. (C) As in (B), except showing interannual anomalies for the control (red) and NoEQ (green) solutions. Trends are removed from all curves.

Interannual ENSO is known to be associated with wind variations within a narrow equatorial band. To see if the detrended component of T'_{eq} is governed by the same equatorial-wave dynamics, we obtained a solution with the wind stress τ split into its 40-year mean climatology $\overline{\tau}$ and deviations from it τ' and with τ' suppressed in a 10°-wide equatorial zone by applying the weight function,

$$f(\theta) = \frac{1}{2}\left\{-\tanh[\frac{3}{5}(\theta+5^{\circ})] + \tanh[\frac{3}{5}(\theta-5^{\circ})]\right\} + 1, \quad (1)$$

where θ is latitude in degrees. Curves of T'_{eq} for the resulting solution (hereafter labeled "NoEQ") are provided in Figs. 2B

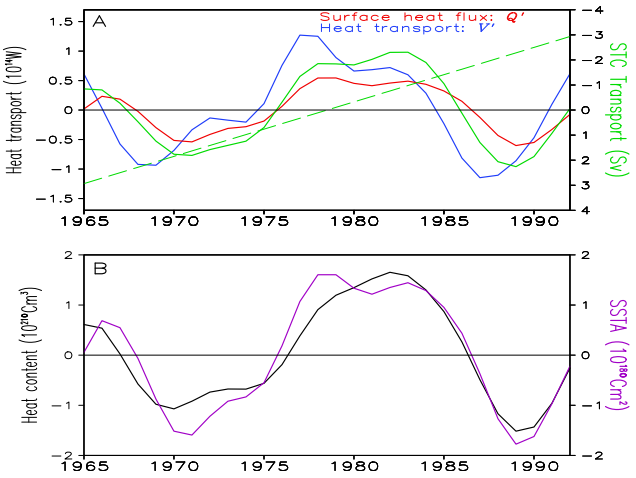

Figure 3. (A) Decadal anomalies of anomalous heat transport $\mathcal{V}'$ (blue line; left axis), area-integrated surface heat flux $\mathcal{Q}'$ (red line; left axis), and STC strength $\Delta\psi'$ (green solid line; right axis) for solution NoEQ. (B) Decadal anomalies of H' (black line; left axis), and SST anomalies averaged over area $\mathcal{A}$ (purple line; right axis) for solution NoEQ. Trends are removed from all curves, with trend of $\Delta\psi'$ plotted in green dashed line in (A). The $\Delta\psi'$ curves are reversed for easy comparison with other curves.

and 2C (green curves), the two panels showing decadal and interannual variability, respectively; the former is obtained by applying a 9-year, weighted, running-mean filter, and the latter is the difference between unfiltered and filtered time series. In comparison to the control run (red curves), solution NoEQ has almost no interannual variability (Fig. 2C). In contrast, its decadal component remains strong, with its amplitude typically decreasing by less than half (Fig. 2B). This difference suggests that decadal variability is governed by different dynamics than interannual ENSO, involving wind variability outside the equatorial wave guide.

To test the influence of midlatitude winds, we obtained another solution forced by a version of the observed winds with neither equatorial nor midlatitude wind variability, the latter implemented by applying weight functions similar to (1) south of 20°S and north of 25°N (the north-south asymmetry resulting from the asymmetry of the winds). Equatorial SSTAs remain nearly identical to those in the NoEQ run, indicating that midlatitude wind variability is unimportant for forcing them.

Finally, to examine the effects of local equatorial wind variations, we forced the model with wind anomalies only near the equator using the inverse weight function, $1-f(\theta)$. This solution (hereafter labeled "EQ") also has a significant decadal T'_{eq} (purple curve in Fig. 2B), with an amplitude almost the same as that in the NoEQ run (green line). In fact, the sum of T'_{eq} curves for the EQ and NoEQ solutions reproduces the curve for the control run very well, indicating that the equatorial SST variability is quite linear in response to wind forcing. Furthermore, it is noteworthy that T'_{eq} for solution EQ leads those in both the control run and solution NoEQ by 1 and 2 years, respectively, as determined by a lagged correlation analysis.

3. Influence of STC variability

The preceding experiments demonstrate that wind variability in the off-equatorial tropics is an effective mechanism for generating equatorial decadal SSTAs. Here, we analyze solution NoEQ to determine how remotely driven effects are communicated to the equator.

A useful diagnostic is the heat-anomaly budget for the tropical upper ocean. It is defined by the volume integral of the model's temperature-anomaly equation in a box that extends across the basin from $y_s = 11°$S to $y_n = 15°$N and from -550 m to the ocean surface. Latitudes y_s and y_n define the boundaries of the tropics in our model; they are the bifurcation latitudes of the model's South and North Equatorial Currents, that is, where the currents divide at the western boundary to flow either poleward to return to the subtropics or equatorward to participate in the STCs. The bottom is deep enough to encompass almost all of the mean STC (Fig. 1). The resulting heat-anomaly equation can be written

$$\frac{dH'}{dt} = \mathcal{V}' - \mathcal{Q}', \tag{2}$$

where H' is the anomalous heat content in the box, $\mathcal{V}'$ is the heat transport into the box through its sides and bottom, $\mathcal{Q}' = \gamma \int\int_{\mathcal{A}} T'_0 dxdy$ is the integral of the surface heat flux out of the box over its horizontal area $\mathcal{A}$, and T'_0 is the solution's SSTA field.

Figure 3A plots $\mathcal{V}'$ (blue curve) and $\mathcal{Q}'$ (red curve) for solution NoEQ. It also plots the strength of the meridional streamfunction anomaly ψ', $M' \equiv \psi'(y_n, z_m) - \psi'(y_s, z_m)$, where $z_m = -20$ m is the depth at which M' attains its maximum value (as for $\overline{\psi}$ in Fig. 1).

The $\mathcal{Q}'$ curve is very similar to decadal T'_{eq} (Fig. 2B; green curve), and to a good approximation $\mathcal{Q}' = bT'_{eq}$, $b = 2.83 \times 10^{14}$ W °C^{-1}. This agreement is not surprising since $\mathcal{Q}'$ is proportional to the average of T'_0 over area $\mathcal{A}$ in our model. As shown in Figure 3B, there is also a close relationship between $\mathcal{Q}'$ and H', with $H' = a\mathcal{Q}'$, $a = 841$ m. The two relations imply that $T'_{eq} = (1/ab)H'$, a clear statement that equatorial SST anomalies are dynamically driven, namely, by vertical shifts in the depth of the thermocline.

The preceding relationships allow (2) to be rewritten for decadal time scales as

$$\frac{dT'_{eq}}{dt} = \frac{1}{ab}\mathcal{V}' - \frac{1}{a}T'_{eq}. \tag{3}$$

According to (3), we interpret T'_{eq} to be forced by $\mathcal{V}'$. If we assume that $\mathcal{V}'$ varies sinusoidally with period P, we can solve (3) analytically. Without $\mathcal{Q}'$, the last term in (3) is absent, and T'_e lags $\mathcal{V}'$ by a quarter cycle. With $\mathcal{Q}'$ and the above value for a, the lag is about 2 years when $P = 10$ years, consistent with the lag of 1–2 years found in the solution (blue and red curves in Fig. 3A) based on a lagged correlation analysis.

It remains to determine the cause of $\mathcal{V}'$. Ignoring the trend in M', there is an obvious close relationship between $-M'$ and $\mathcal{V}'$ in Figure 3A, suggesting that $\mathcal{V}'$ is driven by variations in the STC strength. A lagged cross-correlation analysis, however, shows that $-M'$ lags $\mathcal{V}'$ by 1 to 2 years. In fact, the STC branches do not spin up simultaneously, the surface Ekman layer responding nearly instantaneously to wind variations and the subsurface geostrophic flow adjusting more slowly via the propagation of baroclinic waves [*Klinger et al.*, 2001]. The $\mathcal{V}'$ curve is determined in large part by the fast surface response that drains surface warm water out of the tropics, thereby leading $-M'$.

Theories of ocean circulation suggest that M' is in turn controlled by the zonal wind stress on the boundaries between the subtropics and tropics [*McCreary and Lu*, 1994]. Briefly, in response to an increase in the trades, strengthened Ekman flow transports more warm surface water out of the tropics, which therefore must be compensated by an increased equatorward transport of cool subsurface water, thereby leading to a cooling of equatorial SSTs [*Kleeman et al.*, 1999; *Klinger et al.*, 2001].

4. Summary and Discussion

We have investigated the causes of decadal SST variability in the equatorial Pacific using an ocean GCM driven by observed wind stress. In contrast to interannual SST variability, which is largely forced by changes in the near-equatorial winds, decadal SST variability is driven nearly equally by equatorial winds and off-equatorial winds in the trade-wind bands (20°–8°S and 8°N –25°N). The part of equatorial decadal variability driven by off-equatorial winds is closely related to the strength of the STCs in both hemispheres, consistent with the $V'\overline{T}$ mechanism [*Kleeman et al.*, 1999]. Moreover, the trend of the STC strength (dashed line in Fig. 3A) is also consistent with the observed variability of equatorward geostrophic flow reported by *McPhaden and Zhang* [2001].

Our experiments also show that the STC-induced SSTAs lag roughly two years behind those in response to local equatorial winds. This lag suggests that local forcing by equatorial winds initiates decadal SST anomalies and that remote forcing subsequently maintains and strengthens them. This time lag may be part of the oceanic response to a tropical-wide change in the trade winds as follows. Relaxed easterlies, by rapid equatorial wave adjustment, lead to a deeper thermocline and an SST increase in the eastern equatorial Pacific. The reduced trade winds will further give rise to a delayed equatorial ocean warming by weakening the STCs. Thus, on decadal and longer time scales, the STCs act cooperatively with the ENSO-type equatorial-wave adjustment to cause SST variability in the equatorial Pacific.

The delayed effect of the STCs on SST also suggests that STC variability plays a secondly role in the dynamics of decadal oscillations, acting more to amplify than to initiate them. The cause of the wind variability that drives equatorial decadal variability remained to be determined. Our results, however, are consistent with the hypothesis that T'_{eq} is caused by extratropical modes of decadal variability [*Miller and Schneider*, 2000] that force equatorial wind variations, for example, via atmospheric teleconnections [*Pierce et al.*, 2000].

Acknowledgments. We thank B. Klinger, A. Solomon, S. Minobe, and K. Takeuchi for helpful discussions, and A. Lazar and G. Speidel for comments. This study was supported by the Frontier Research System for Global Change through its support of the International Pacific Research Center (IPRC). The manuscript is IPRC contribution #118 and SOEST contribution #5869.

References

Alexander, M., I. Blade, M. Newman, J. Lanzante, N.-C. Lau, and J. Scott, The Atmospheric Bridge: the Influence of ENSO Teleconnections on Air-Sea Interaction Over the Global Oceans, *J. Climate*, submitted, 2001.

An, S.-I. and B. Wang, Interdecadal Change of the Structure of the ENSO Mode and Its Impact on the ENSO Frequency, *J. Climate*, *13,* 2044–2055, 2000.

Deser, C., M. A. Alexander, and M. S. Timlin, Upper-Ocean Thermal Variations in the North Pacific during 1970–1991, *J. Climate*, *9,* 1840-1855, 1996.

Fedorov, A. V., and S. G. Philander, Is El Nino Changing?, *Science*, *288,* 1997-2002, 2000.

Gu, D., and S. G. H. Philander, Interdecadal Climate Fluctuations That Depend on Exchanges Between the Tropics and Extratropics, *Science*, *275,* 805-807, 1997.

Inui, T., A. Lazar, A. Busalacchi, P. Malanotte-Rizzoli, and L. Wang, Wind Stress Effect on the Subtropical-Tropical Circulation in the Atlantic, *J. Phys. Oceanogr.*, submitted, 2001.

Kalnay, E., *et al.*, The NCEP/NCAR 40-year reanalysis project, *Bull. Amer. Meteor. Soc.*, *77,* 437-471, 1996.

Klinger, B. A., J. P. McCreary, and R. Kleeman, The Relationship Between Oscillating Subtropical Wind and Equatorial Temperature, *J. Phys. Oceanogr.*, in press, 2001.

Kleeman, R., J. P. McCreary, and B. A. Klinger, A mechanism for generating ENSO decadal variability, *Geophys. Res. Lett.*, *26,* 1743-1746, 1999.

Liu, Z., A simple model of the mass exchange between the subtropical and tropical ocean, *J. Phys. Oceanogr.*, *24,* 1153-1165, 1994.

McCreary, J. P., and P. Lu, Interaction between the subtropical and equatorial ocean circulations: The subtropical cell, *J. Phys. Oceanogr.*, *24,* 466-497, 1994.

McPhaden, M. J., and D. Zhang, Decadal Spin-down of the Pacific Ocean Shallow Meridional Overturning Circulation, *Nature*, submitted, 2001.

Miller, A. J., and N. Schneider, Interdecadal climate regime dynamics in the North Pacific Ocean: theories, observations and ecosystem impacts, *Progress in Oceanogr.*, *47,* 355-379, 2000.

Nonaka, M., and S.-P. Xie, Propagation of North Pacific interdecadal subsurface temperature anomalies in an ocean GCM, *Geophys. Res. Lett.*, *27,* 3747-3750, 2000.

Pierce, D. W., T. P. Barnett, and M. Latif, Connections between the Pacific Ocean tropics and midlatitudes on decadal time scales, *J. Climate*, *13,* 1173-1194, 2000.

Schneider, N., S. Venzke, A. J. Miller, D. W. Pierce, T. O. Barnett, C. Deser, and M. Latif, Pacific thermocline bridge revisited, *Geophys. Res. Lett.*, *26,* 1329-1332, 1999.

Timmermann, A., and F.-F. Jin, A nonlinear Mechanism for Decadal El Niño Amplitude Changes, *Geophys. Res. Lett.*, in press, 2001.

Xie, S.-P., T. Kunitani, A. Kubokawa, M. Nonaka, and S. Hosoda, Interdecadal Thermocline Variability in the North Pacific for 1958-1997: A GCM Simulation, *J. Phys. Oceanogr.*, *30,* 2798-2813, 2000.

Zhang, R.-H., L. M. Rothstein, and A. J. Busalacchi, Origin of warming and El Nino change on decadal scales in the tropical Pacific Ocean, *Nature*, *391,* 879-883, 1998.

Zhang, Y., J. M. Wallace, and D. S. Battisti, ENSO-like decadal variability over the Pacific sector, *J. Climate*, *10,* 1004-1020, 1997.

J. P. McCreary, M. Nonaka, and S.- P. Xie IPRC/SOEST, University of Hawaii, 2525 Correa Road, Honolulu, Hawaii 96822. (e-mail: jay@soest.hawaii.edu; nona@soest.hawaii.edu; xie@soest.hawaii.edu)

(Received June 29, 2001; revised September 29, 2001;
accepted October 8, 2001.)